Science Bulletin 64 (2019) 1011–1017

Contents lists available at ScienceDirect

Science Bulletin

journal homepage: www.elsevier.com/locate/scib

Science Bulletin
www.scibull.com

Article

Abnormal expression of miR-331 leads to impaired heart function

Jin-Jing Zhang [a], Li-Peng Wang [b], Rong-Chang Li [b], Meng Wang [c], Zeng-Hui Huang [c,d], Min Zhu [a], Jia-Xing Wang [a], Xiu-Jie Wang [c,d], Shi-Qiang Wang [b,*], Ming Xu [a,*]

[a] Department of Cardiology, Institute of Vascular Medicine, Peking University Third Hospital, NHC Key Laboratory of Cardiovascular Molecular Biology and Regulatory Peptides, Key Laboratory of Molecular Cardiovascular Science, Ministry of Education, Beijing Key Laboratory of Cardiovascular Receptors Research, State Key Laboratory of Natural and Biomimetic Drugs, Peking University, Beijing 100191, China
[b] State Key Laboratory of Membrane Biology, College of Life Sciences, Peking University, Beijing 100871, China
[c] Institute of Genetics and Developmental Biology, Chinese Academy of Sciences, Beijing 100101, China
[d] University of Chinese Academy of Sciences, Beijing 100049, China

ARTICLE INFO

Article history:
Received 16 March 2019
Received in revised form 23 April 2019
Accepted 30 April 2019
Available online 22 May 2019

Keywords:
MiR-331
Excitation-contraction coupling
Junctophilin 2
Heart function

ABSTRACT

MicroRNAs (miRNAs) play important roles in maintaining normal heart function. Abnormal expression of miR-331 has been observed in the hearts of patients with atrial fibrillation and Marfan syndrome. However, whether miR-331 regulates cardiac function under physiological and pathological conditions still remains unknown. In the present study, we investigated the function and underlying mechanisms of miR-331 in a pressure overload-induced heart failure model and miR-331 transgenic rat model. First, we found that the expression of miR-331-3p exhibited a 1.7-fold increase in hypertrophy compared with that in the sham group ($P < 0.01$), yet the expression of miR-331-5p remained unchanged. Furthermore, overexpression of miR-331 in cardiomyocytes and defective excitation-contraction (E-C) coupling efficiency were observed. Luciferase assays showed that miR-331-3p suppressed JPH2 expression by binding to the coding region of JPH2 mRNA. Finally, in the miR-331 transgenic rat model, JPH2 expression was suppressed at both the mRNA and protein levels in vivo, which resulted in impairment of both the E-C coupling efficiency of cardiomyocytes and systolic function of the heart. This finding mechanistically linked miR-331 to JPH2 downregulation and suggested an important role for the abnormal expression of miR-331 leading to the dysfunction of E-C coupling in heart failure.

1. Introduction

MicroRNAs (miRs) play important roles in the cardiovascular system [1]. Thus, the precise expression control of miRNAs is vital to maintain normal heart function. Abnormal expression of miR-331 was noticed in atrial fibrillation patients [2] and Marfan syndrome patients without mitral valve prolapse (MVP) [3]. However, the biological function of miR-331 and its potential targets in the heart remain obscure.

One strategy to prevent heart failure is to stop or postpone the transition of hypertrophy from the compensated stage to the decompensated stage [4]. The underlying mechanisms of excitation-contraction (E-C) coupling regulation have been studied extensively in the compensated stage of hypertrophy [5], yet few miRNAs related to this process have been identified so far. Therefore, exploring more miRNAs involved in cardiac hypertrophy is important for developing clinical therapies against heart failure.

JPH2 (Junctophilin 2) is a structural protein linking the SR (sarcoplasmic reticulum) to the TT (T-tubule) on the cell membrane and plays a key role in signaling between LCCs (L-type Ca^{2+} channel) and RyRs (ryanodine receptors) during E-C coupling [6]. It is also a participant in a self-protective mechanism in the stressed heart [7]. JPH2 knockdown turns to disrupt the TT system and E-C coupling maturation, reduce the volume density and spatial span of TT-SR junctions, and decrease the efficiency of E-C coupling [8–10]; the downregulation of JPH2 is potentially a common mechanism underlying the defective E-C coupling in heart failure. In the present study, we showed that increased expression of miR-331 downregulated JPH2 and impaired E-C coupling in cardiomyocytes in a pressure overload-induced heart failure rat model and miR-331 transgenic rat model. Our findings provided new molecular insights into the microRNA-mediated dysfunction of E-C coupling during the pathogenesis leading to heart failure.

* Corresponding authors.
E-mail addresses: wsq@pku.edu.cn (S.-Q. Wang), xuminghi@bjmu.edu.cn (M. Xu).

https://doi.org/10.1016/j.scib.2019.05.017
2095-9273/

2. Methods

2.1. Cell culture

HEK-293A cells were cultured in high-glucose Dulbecco's modified eagle medium supplemented with 10% fetal bovine serum (HyClone) and 1% penicillin and streptomycin (Life Technologies) at 37 °C in a humidified incubator containing 5% CO_2.

2.2. Neonatal rat cardiomyocytes culture

Neonatal rat cardiomyocytes were isolated and cultured. Cardiomyocytes were dissociated from the ventricles of <48 h old neonatal Sprague-Dawley rats using 0.1% trypsin (HyClone) and 80 U/mL collagenase (Worthington Biochemical Corp) in Hank's balanced salt solution (calcium-free; HyClone). To purify the cardiomyocytes from nonmyocytes, isolated cells were preplated in high-glucose Dulbecco's modified eagle medium supplemented with 10% fetal bovine serum and 1% penicillin and streptomycin at 37 °C in a humidified incubator containing 5% CO_2 for 120 min. The enriched cardiomyocyte fractions were seeded into 3.5 cm culture dishes and cultured under the same conditions. The culture medium was changed to serum-free or full medium as appropriate, and the cells were cultured for another 8 h before further experiments.

2.3. Animal preparation

All applicable institutional and/or national guidelines for the care and use of animals were followed. Animal experiments were approved by the Institutional Animal Care and Use Committee of Peking University. A model of heart failure induced by pressure overload was created by performing TAC (transverse aortic constriction) surgery in male Sprague-Dawley rats (body weight, 50–55 g) as described previously [8]. Briefly, rats were anesthetized with a ketamine-xylazine mixture (5:3, 1.32 mg/kg i.p.). After pedal pinch reflexes were completely inhibited, we opened the thorax of the rat and put a silver clip (0.9 mm inside diameter) on the ascending aorta in the TAC group but not in the sham group. To characterize the state of heart failure, the echocardiograph was measured using a VisualSonics Vevo 2100 cardiovascular ultrasound system.

miR-331 transgenic rats were constructed by Viewsolid Biotech Company. The miR-331-expressing transgenic vector was constructed by ligating the pri-miR-331 fragment into the expressing plasmid, which was linearized by BstEII. The linearized transgenic plasmid DNA was injected into the pronucleus of fertilized eggs. A minimum of 150 one-cell embryos were injected and transferred into at least two pseudopregnant rats to produce transgenic rats. Subsequently, the founder rats were born and genotyped by qPCR to verify the overexpression of miR-331-3p (Fig. S1 online). Two founder rats with higher miR-331-1p expression were bred separately with wild type SD rats until F2 rats were obtained.

2.4. Small RNA northern-blot hybridization

Small RNA northern-blot hybridization was carried out following previously reported procedures [11] using 20 μg of total RNA in each experiment. The complementary sequences of miRNAs were labeled by [γ-32P]ATP and used as probes.

2.5. Isolation of adult rat cardiomyocytes

The hearts of SD rats at 8 weeks were rapidly removed under 5% isoflurane anesthesia and mounted on a Langendorff apparatus. The heart was then perfused for 5 min at 37 °C with a Ca^{2+} free Tyrode's solution containing (in mmol/L): 135 NaCl, 4 KCl, 1 $MgCl_2$, 1.2 NaH_2PO_4, 11.9 $NaHCO_3$, 10 glucose, and 10 taurine saturated with 95% O_2 and 5% CO_2. Collagenase type II (0.7 mg/mL) was then added to the perfusate, and ventricular cardiac myocytes were enzymatically isolated. After 15–20 min, the heart was taken down, and the ventricle was cut into small pieces. Finally, the myocytes were centrifuged and resuspended in Tyrode's solution containing 1 mmol/L Ca^{2+}.

2.6. Echocardiography

Echocardiography was performed with a Vevo 2100 system (VisualSonics, Toronto, Canada). Briefly, rats were placed in an airtight box exposed to 3% isoflurane (Baxter Healthcare, New Providence, RI, USA) to induce anesthesia. After the righting reflex disappeared, the rats were removed from the box and fixed on a heated platform with their nose placed in a small nose cone for isoflurane inhalation. The body temperature of the rats was maintained at 37 °C throughout the procedure to minimize HR variation. The chests of the rats were shaved and cleaned using a depilatory cream (Nair, TMG-255, USA). Warm ultrasound gel was applied to the scan head, which was placed on the chest. The isoflurane concentration was decreased to 1%. When physiological values (especially HR) became stable, two-dimensional parasternal short-axis imaging at the level of the papillary muscle was used as a guide to obtain a left ventricular M-mode tracing. All measurements were averaged from three continuous cardiac cycles per loop. Values for LV end-diastolic volume (LVEDV), LV end-systolic volume (LVESV), ejection fraction (EF), and fractional shortening (FS) were derived automatically by the Vevo 2100 system.

2.7. Dual-luciferase reporter assay

HEK-293A cells were seeded in 24-well plates with complete medium for 24 h before transfection. The 3′-untranslated region (UTR) containing the putative microRNA binding site or G/T mutant sequence and target mutation sequence (which was designed based on the human target gene mRNA sequence in GenBank) was inserted downstream of the firefly luciferase reporter (Shanghai Genechem Co, Ltd, China). The cultures were transiently cotransfected with 5 pmol microRNA agomir and 100 ng firefly luciferase vector (contained either WT or two mutant sequences), together with 50 ng Renilla luciferase vector (served as internal control) via Invitrogen TM Lipofectamine® 3000 (Thermo Fisher Scientific Inc. Beijing, China). Penicillin-free medium was used, and cells were then incubated at 37 °C in a 5% CO_2 incubator for 24 h prior to testing, according to the manufacturer's instruction. The luciferase activities were measured using the Dual-Luciferase Reporter Assay Kit according to the manufacturer's instruction. Three repeated wells were included for each sample to decrease random errors.

2.8. RNA extraction and quantitative real-time PCR

Total RNA was extracted from cells using the Trizol reagent (Invitrogen), according to the manufacturer's instructions. The microRNA cDNA was synthesized using the first-strand reverse transcriptase kit (Tiangen). cDNA was synthesized by the reverse transcription system (Promega), in which each reaction contained 1 μg total RNA, per the manufacturer's instructions. Quantitative RT-PCR gene expression analysis was performed on triplicate samples with SYBR green (Tiangen) technology using a two-step program, and the cycling program was as follows: 94 °C for 2 min, followed by 40 cycles at 94 °C for 20 s, 60 °C for 34 s, followed by a dissociation step to ensure amplification specificity. The primers used in this study are shown in Table S1 (online). The data were

normalized to U6 expression, and the relative gene expression was calculated by $2^{-\Delta\Delta Ct}$.

2.9. Western blot

Total protein from the heart tissues or cells was extracted by RIPA lysis buffer (Solarbio, R0010, China) containing phenylmethanesulfonyl fluoride. For electrophoresis analysis, 20 μg of total protein were electrophoresed, and the gels were transferred to nitrocellulose membranes at 200 mA for 90 min in a transfer buffer (48 mmol/L Tris, 39 mmol/L glycine, and 20% methanol). The blot was washed for 10 min in Tris-buffered saline (TBST) (0.5 mol/L NaCl, 20 mmol/L Tris, and pH 7.5), followed by 1 h of incubation in blocking solution (TBST plus 10% skim milk, fraction V). After incubation, the blot was washed three times for 5 min with TBST and incubated overnight at 4 °C with the following antibodies: anti-GAPDH antibody diluted 1:2,000 and anti-JPH2 antibody diluted 1:1,500. The blot was washed three times and then incubated for 1 h in antibody solution containing fluorescent secondary anti-mouse IgG or anti-rabbit IgG diluted 1:10,000. Finally, the blot was washed and observed using an Infrared Imaging System (Licor Odyssey).

2.10. Whole-cell patch clamp

Isolated cardiomyocytes were bathed in Tyrode's solution containing the following (in mmol/L): 137 NaCl, 4.0 KCl, 1.0 $CaCl_2$, 1.2 $MgCl_2$, 1.2 NaH_2PO_4, 10 glucose, 0.02 tetrodotoxin, and 10 HEPES and 4.0 4-aminopyridine, pH 7.35 adjusted with NaOH. For I_{Ca} (whole-cell Ca^{2+} current through L-type Ca^{2+} channels) and calcium transient recordings, the pipette solution contained the following (in mmol/L): 110 CsCl, 6 $MgCl_2$, 5 Na_2ATP, 15 TEA-Cl and 10 HEPES and 0.2 fluo-4 pentapotassium salt, pH 7.2 adjusted with CsOH. Pipettes with a resistance of 2–3 MΩ were used. The L-type channel current was elicited by 1-s depolarization from a holding potential of −70 mV (to different test potentials (up to +70 mV)) using an Axon 200B amplifier.

Calcium transients were measured using Zeiss LSM-710 confocal microscopy. The calcium level was reported as $\Delta F/F0$, where $F0$ is the resting or diastolic fluo-4 fluorescence. Line scan images were acquired at 3.84 ms/line for whole-cell recording. All experiments were performed at room temperature.

2.11. Statistical analysis

Results were expressed as the mean ± SD or mean ± SE, and statistical analysis was carried out with SPSS 19.0 (IBM Corp, Armonk, NY, USA). Student's *t*-test was used for two groups, one-way or two-way ANOVA was applied for three or more groups, and non-parametric tests were used when the variables were not normally distributed. A value of $P < 0.05$ was considered significant.

3. Results

3.1. miR-331-3p was upregulated in pressure overload-induced cardiac hypertrophy

TAC surgery was used to construct the rat cardiac hypertrophy model, and echocardiography at 8 weeks after surgery revealed that the thickness of the left ventricle's posterior wall was significantly increased (Fig. 1a). We analyzed the expression profiles of miR-331-3p in rat hearts using small RNA northern-blot hybridization. The results showed that miR-331-3p expression increased significantly in cardiac hypertrophy (Fig. 1b). Furthermore, the levels of two mature miR-331s, miR-331-3p and miR-331-5p, were determined by real-time qPCR. As shown in Fig. 1c, miR-331-3p expression increased by ~60% ($P = 0.002$). However, no significant difference in miR-331-5p expression was found between the sham and TAC groups (Fig. 1d). These data suggested that miR-331-3p was involved in cardiac hypertrophy.

3.2. Overexpression of miR-331 led to defective E-C coupling efficiency in cardiomyocytes

To detect the effects of miR-331 on cardiomyocytes, miR-331 adenoviral vectors containing GFP or miR-331 precursor sequences were constructed and transfected into the cardiomyocytes of adult rats. To quantify the efficiency of excitation-contraction (E-C) coupling at the cellular level, we combined whole-cell patch clamp experiments with confocal imaging and recorded the intracellular Ca^{2+} transients in transfected cardiomyocytes during depolarization of the cell membrane from −70 mV to various voltages (Fig. 2a). Although miR-331 overexpression did not influence the L-type calcium current (I_{Ca}) (Fig. 2b), it significantly reduced the calcium transient amplitude (Fig. 2c). The gain of E-C coupling, defined as the amplitude of the Ca^{2+} transient per unit I_{Ca}, decreased significantly (Fig. 2d). These results indicated that miR-331 overexpression led to defective E-C coupling.

3.3. Overexpression of miR-331-3p decreased JPH2 expression through binding to the code regain of JPH2 mRNA

To explore the mechanism by which miR-331-3p regulates cardiac hypertrophy, we used miRanda software (http://www.microrna.org) to predict the targets of miR-331-3p. A total of 357 potential targets were predicted for miR-331-3p. Among these, 6 potential target mRNAs were reported to be directly associated with E-C coupling (Fig. 3a). We examined the expression levels of these 6 potential target mRNAs in cardiomyocytes with overexpression of miR-331-3p by qPCR. The results showed that the mRNA level of JPH2 was significantly downregulated in the miR-331-3p overexpression group (Fig. 3b), and the protein level of JPH2 was also significantly decreased (Fig. 3c).

Two potential binding sites of miR-331-3p were identified in JPH2 mRNA (one in the 3′-UTR and one in the coding region) using bioinformatics prediction. Luciferase reporter assays were further used to identify the binding site between miR-331-3p and JPH2 (Fig. S2 online). Unexpectedly, the luciferase activity of the plasmid constructed with the 3′-UTR of JPH2 was not significantly changed by miR-331-3p (Fig. 3d). However, the luciferase activity of the plasmid constructed with the potential miR-331-3p binding site located within the coding region of JPH2 mRNA was significantly downregulated by miR-331-3p (Fig. 3e), and the sequence of the coding region miR-331-3p target site was conserved between rno-JPH2 and has-JPH2 mRNAs (Fig. S2 online). This inhibited effect was abolished by the mutation of binding sites in the coding region of JPH2 (Figs. 3e, S3 online). These results proved that miR-331-3p suppressed JPH2 expression depended on the coding region target sequences.

3.4. miR-331 transgenic rats exhibited impaired heart function and decreased JPH2 expression

To study the effects of miR-331 on heart function, transgenic rats with overexpression of miR-331 were constructed; 7-month-old rats were sacrificed after being anesthetized. No significant difference was found with respect to heart rate, blood pressure, serum biochemical parameters, heart weight-to-body weight ratio, and heart weight-to-tibia length ratio between wild type and miR-331 transgenic rats (TG line 1 and line 2) (Tables S1–S3 online). The results of qPCR revealed that the expression of miR-331-3p in two

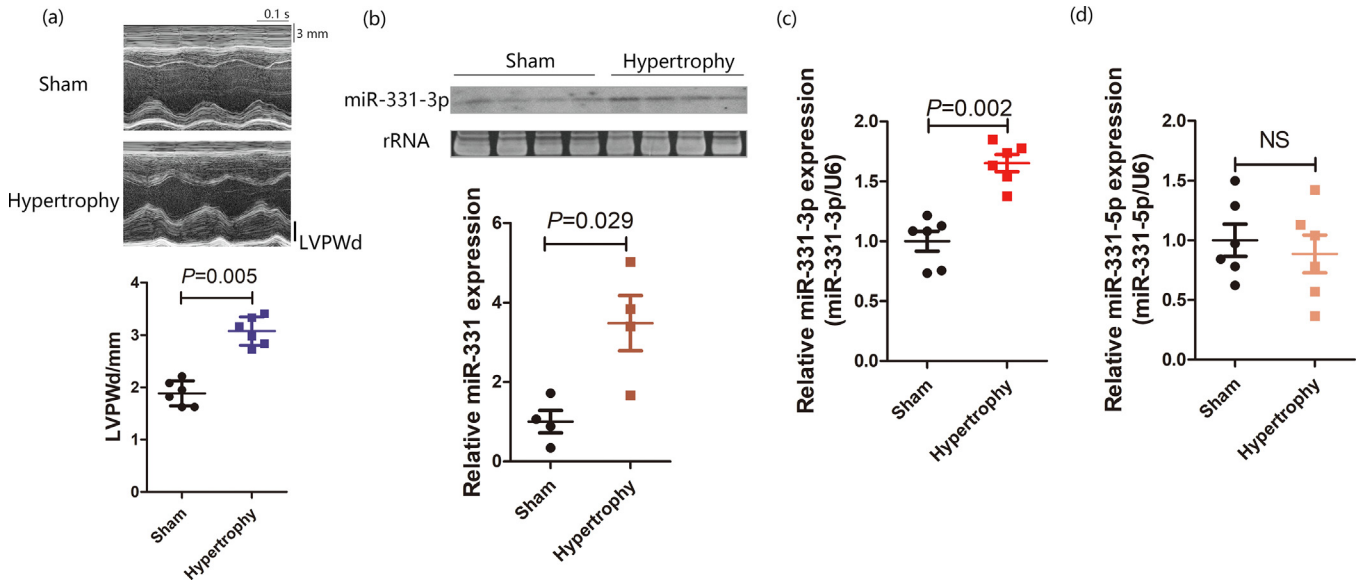

Fig. 1. (Color online) miR-331 upregulation in cardiac hypertrophy model. (a) Echocardiography revealed the increase of left ventricular posterior wall thickness (LVPWd) in TAC rats (mean ± SE; unpaired two-tailed Student's *t* test, $n = 6$). (b) Northern blot analysis of miR-331-3p (mean ± SE; unpaired two-tailed Student's *t* test, $n = 4$). (c) Quantitative analysis of miR-331-3p level by qPCR (mean ± SE; unpaired two-tailed Student's *t* test, $n = 6$). (d) Quantitative analysis of miR-331-5p level by qPCR in cardiac hypertrophy model. (mean ± SE; NS, not significant, unpaired two-tailed Student's *t* test, $n = 6$).

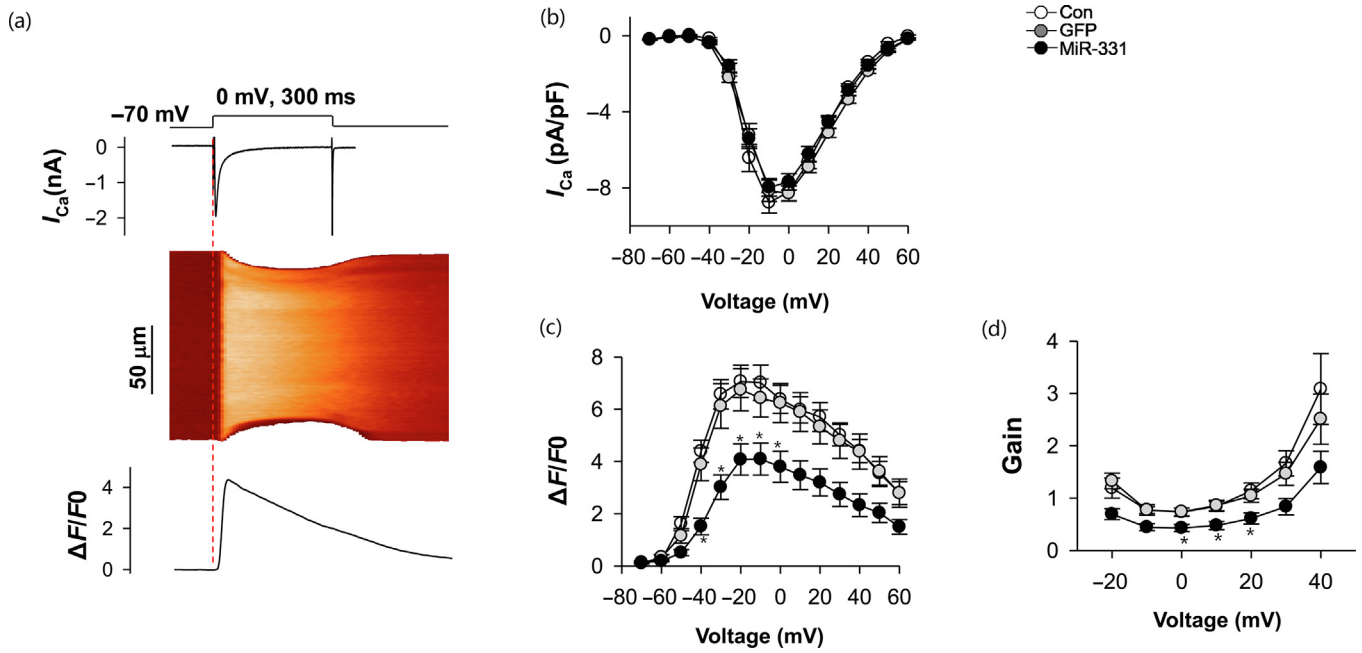

Fig. 2. (Color online) Overexpressed miR-331 leads to defective excitation-contraction (E-C) coupling efficiency in rat ventricular myocytes. (a) Representative whole-cell patch clamp recordings (upper panels) and confocal images (lower panels) when the membrane potential was depolarized to 0 mV. Voltage dependence of I_{Ca} density (b) and Ca^{2+} transient amplitude (c) in control, GFP, and miR-331. (d) Gain of E-C coupling was calculated as the Ca^{2+} transient amplitude per unit I_{Ca} density at 0 mV. (mean ± SE; $^*P < 0.05$ versus control group, one-way ANOVA with Tukey's *post hoc* test, $n \geq 13$ in each group).

TG lines were both increased, as TG line 1 exhibited a 1.78-fold increase and TG line 2 exhibited a 1.85-fold increase compared to wild-type rats (Fig. 4a). Fractional shortening (FS) and left ventricular ejection fraction (LVEF) (Fig. 4b) were significantly reduced in the miR-331 transgenic rats. Moreover, the mRNA level and protein level of JPH2 decreased in the cardiac tissue of miR-331 transgenic rats (Fig. 4c, d). These data suggested that the decreased JPH2 expression underlying the impaired heart function of miR-331 transgenic rats.

3.5. Cardiomyocytes isolated from miR-331 transgenic rats showed impaired E-C coupling efficiency

To detect the underlying mechanism of cardiac dysfunction of miR-331 transgenic rats, the E-C coupling efficiency was measured at the cellular level (Fig. 5a). The results showed that calcium current from LCCs was similar between the wild-type and transgenic groups (Fig. 5b). However, the global Ca^{2+} transient, gain of E-C coupling and fractional shortening of cardiomyocytes

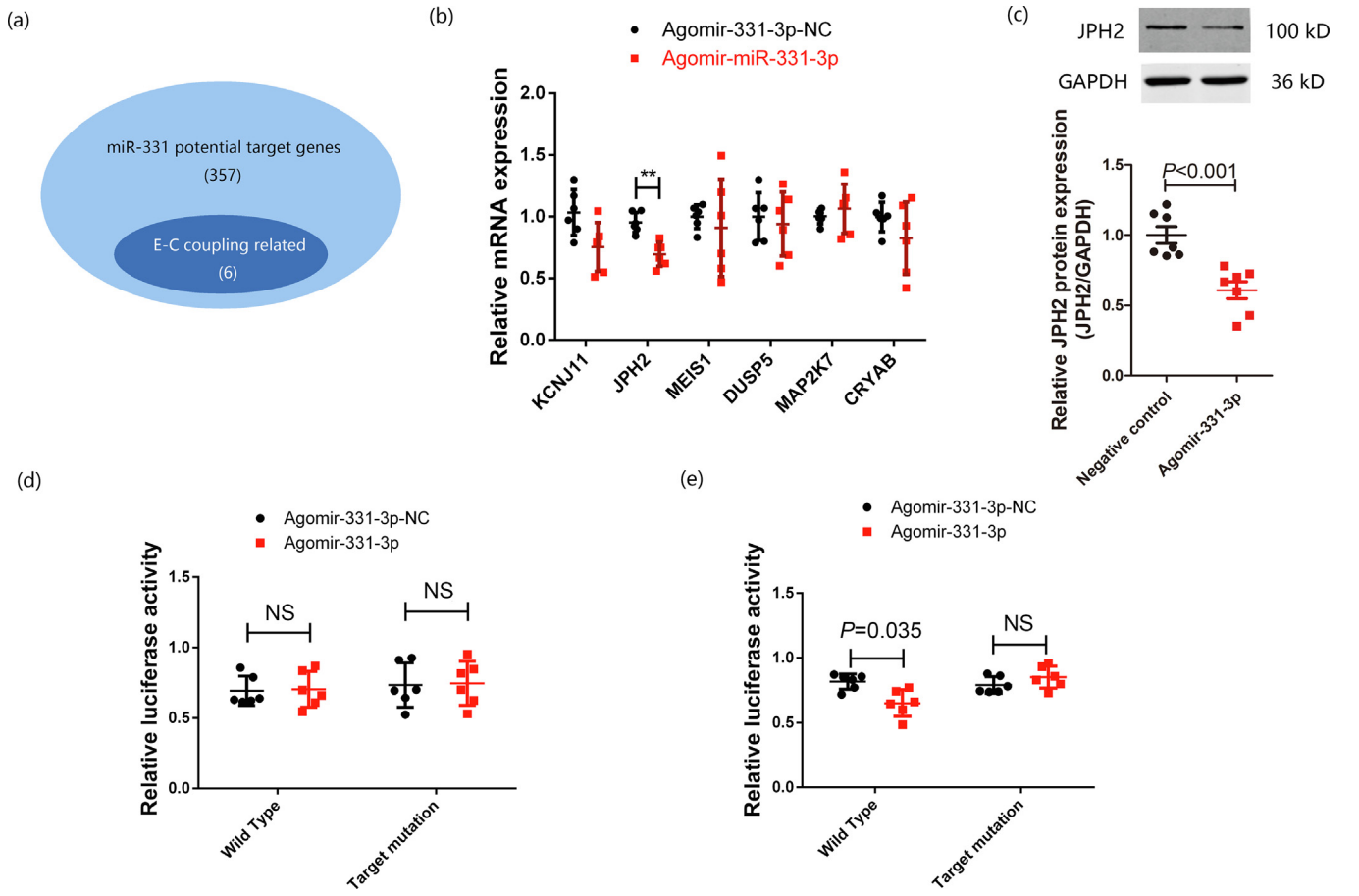

Fig. 3. (Color online) miR-331 inhibited JPH2 expression by binding to its coding region Candidate target gene (a) and mRNA expression after miR-331 transfection (b) (mean ± SD; $^{**}P < 0.01$ vs. negative control group, unpaired two-tailed Student's *t* test, $n = 6$). (c) JPH2 protein expression in miR-331-3p overexpressed neonatal rat cardiomyocytes (mean ± SD; unpaired two-tailed Student's *t* test, $n = 6$). (d) Luciferase reporter assay of miR-331 3′UTR binding sites (mean ± SD; two-way ANOVA with Tukey's *post hoc* test, $n = 6$). (e) Luciferase reporter assay of miR-331 coding region binding sites. (mean ± SD; two-way ANOVA with Tukey's *post hoc* test, $n = 6$).

were significantly lower in both transgenic groups (Fig. 5c), leading to a decreased gain of E-C coupling (Fig. 5d) and reduced fraction of cell contraction (Fig. 5e). These results provided firm evidence that miR-331 is an important regulator of cardiac E-C coupling.

4. Discussion

In the present study, we found that miR-331-3p was upregulated in cardiac hypertrophy. To further investigate the roles of miR-331-3p in cardiac function, we constructed a miR-331 transgenic rat model. The expression level of miR-331-3p in transgenic rats was comparable to that in the heart hypertrophy model. Transgenic rats showed impaired cardiac function with decreased LV ejection fraction and fraction shortening. Isolated cardiomyocytes showed impaired E-C coupling efficiency with elevated levels of miR-331-3p. The results suggested that abnormal expression of miR-331-3p was related to cellular E-C uncoupling and the cardiac systolic function of rats. Therefore, we will focus on its underlying mechanism in E-C coupling.

Since microRNAs exert their biological effects through binding to multiple target genes [12–14], bioinformatic methods were used to predict its potential target genes [15]. We sought out 6 target genes that are related with E-C coupling (Fig. 3a). Furthermore, we overexpressed miR-331-3p in neonatal rat cardiomyocytes and detected the expression of these six genes at the mRNA level, of which only JPH2 expression was downregulated (Fig. 3b). On the other hand, the factors underlying E-C coupling efficiency include sarcoplasmic reticulum (SR). RyRs sensitivity [16], SERCA function [17,18] as well as T-tubule structure [19]. In the present study, miR-331-3p was not predicted to bind either RyR2 or SERCA mRNA. In contrast, the miR-331-3p binding site on JPH2, which encodes a structural protein coupling SR to T-tubule [20], was confirmed by luciferase assay. It was previously reported that JPH2 downregulation was related to atrial fibrillation [21], which may also explain the significance of increased miR-331 in atrial fibrillation. However, as many other factors are involved in regulating heart remodeling [22], arrhythmias [23] and intracellular Ca^{2+} [24], we cannot exclude that there are still many unknown genes regulated by miR-331-3p that may play roles in impaired E-C coupling. Therefore, JPH2 rescue experiments are needed for further study.

The main finding of the present study is impaired systolic function in miR-331 transgenic rats (Fig. 4b). In addition to impaired E-C coupling, apoptosis of cardiomyocytes needs is also a concern. Studies have shown that miR-331 could bind to its target genes, including HER2 [25–27], VHL [28], and E2F1 [29] (prompting cell proliferation or cell migration and invasion in several cancer types, such as breast cancer, liver cancer, urothelial carcinoma, and cervical cancer). Among these targets, E2F1 is related to cardiomyocyte apoptosis [30]. Its expression level was downregulated in miR-331 transgenic rats. This might explain the phenotypes of increased LV volume and decreased wall thickness in the present study (Table S4 online).

This study demonstrated that miR-331 overexpression led to abnormal cardiac function, partly by repressing JPH2 expression. This research provides a new point for miR-331 function in the cardiovascular system and offered new insight into JPH2 regulation.

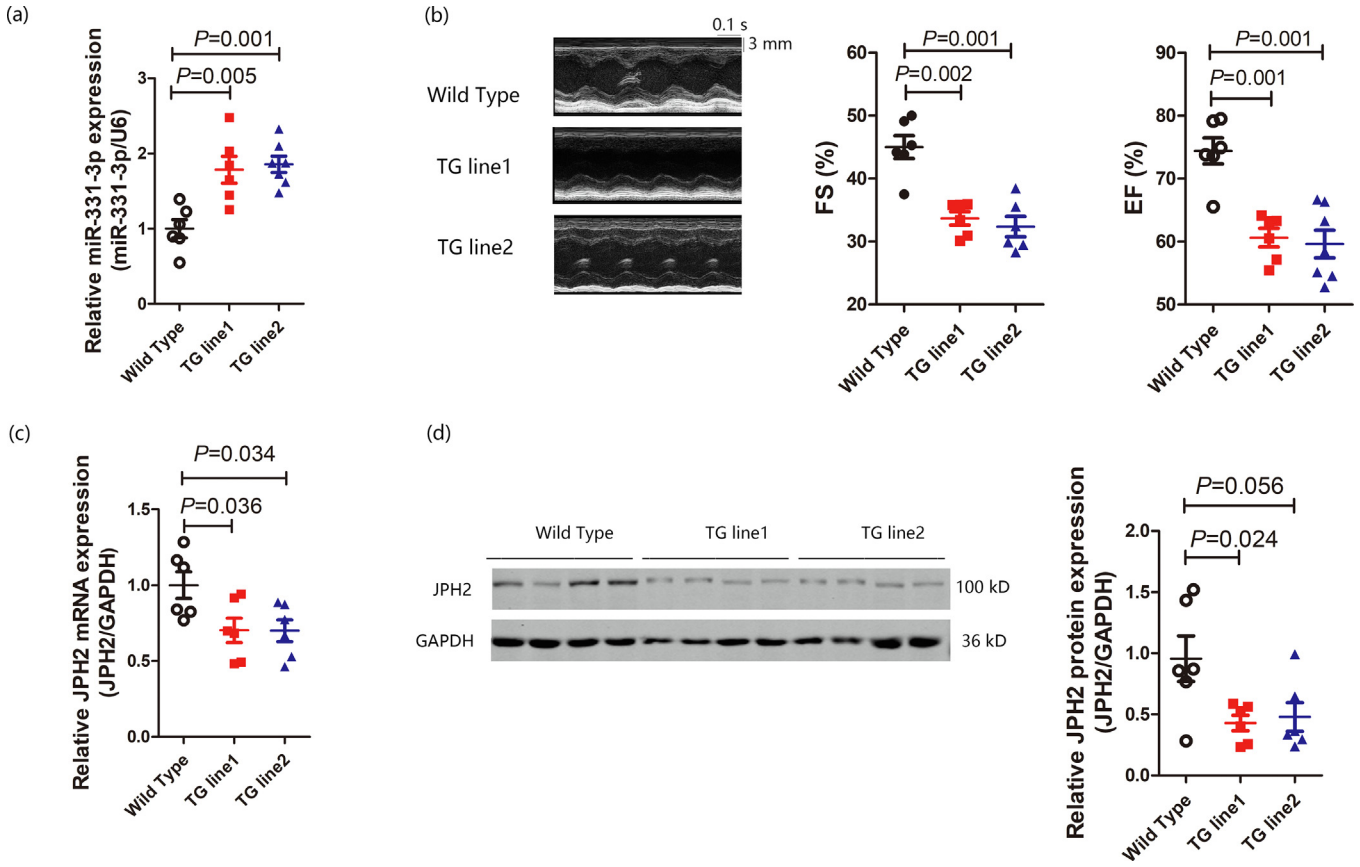

Fig. 4. (Color online) miR-331 overexpression transgenic rats showed impaired heart function (a) miR-331-3p expression in rat heart. (b) Representative M-mode echocardiograph of three groups, and fractional shortening (FS) and left ventricular ejection fraction (LVEF) in three groups measured by echocardiography. (c,d) JPH2 expression at mRNA and protein levels in transgenic rat heart tissue. (mean ± SE; one-way ANOVA with Tukey's *post hoc* test, $n = 6$).

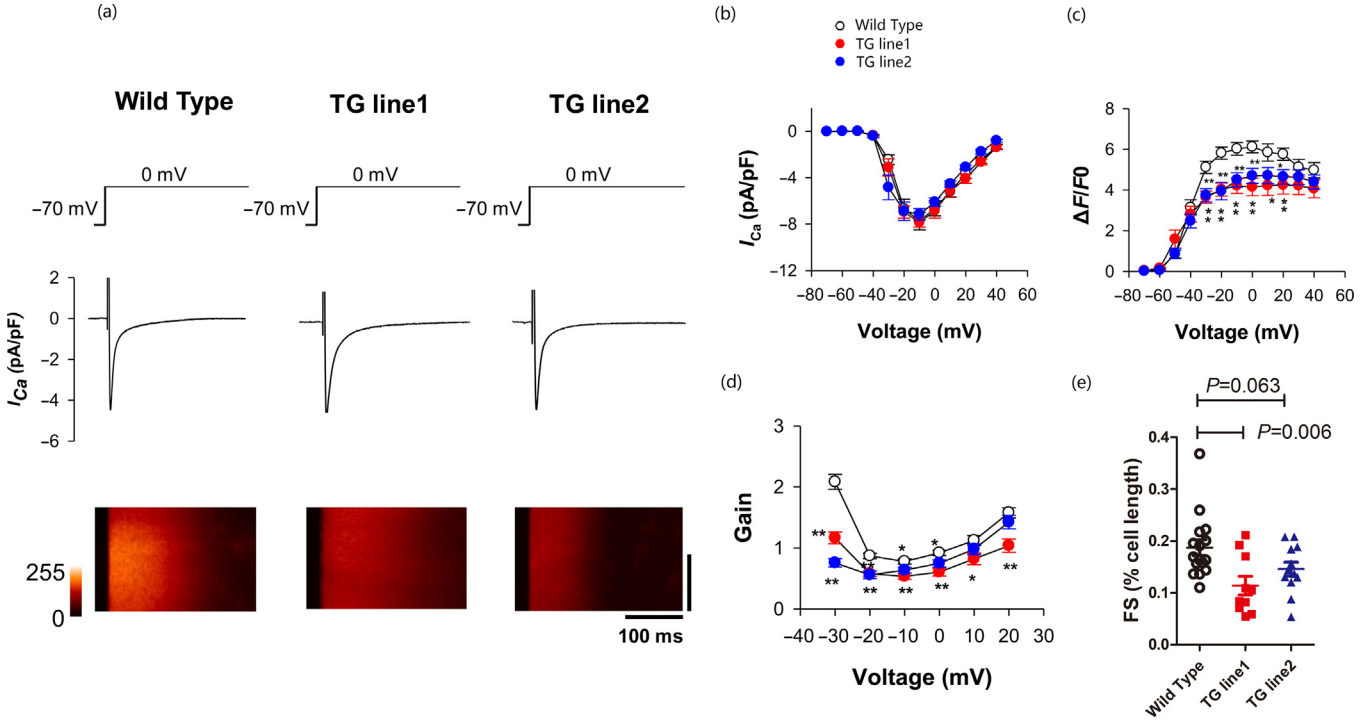

Fig. 5. miR-331 overexpression transgenic rats showed impaired E-C coupling efficiency (a) Typical recordings of LCC calcium currents (I_{Ca}, upper plots) and calcium transients (lower images) in wild type rats and two lines of miR-331 overexpression rats, TG line 1 and TG line 2. Voltage dependence of I_{Ca} density (b) and Ca^{2+} transient amplitude (c) in control, GFP, and miR-331. (d) Gain of E-C coupling was calculated as the Ca^{2+} transient amplitude per unit I_{Ca} density at 0 mV. (e) Fractional shortening of cardiomyocytes measured by cell edge detection of Ca^{2+} transients at 0 mV. (mean ± SE; $^{*}P < 0.05$, $^{**}P < 0.01$ versus wild type group, one-way ANOVA with Tukey's *post hoc* test; data from ≥18 cells from 3 animals in each group).

Conflict of interest

The authors declare that they have no conflict of interest.

Acknowledgments

This work was supported by the National Natural Science Foundation of China (81625001, 91854209, 31630035) and the National Key Research & Development Program of China (2018YFC1312700, 2018YFC1312701). We also wish to thank Yan Bai for professional technical support.

Author contributions

Ming Xu and Shi-Qiang Wang conceived and designed the experiments. Jin-Jing Zhang, Li-Peng Wang, Rong-Chang Li, Zeng-Hui Huang and Meng Wang performed the experiments. Jin-Jing Zhang, Min Zhu, Jia-Xing Wang, Xiu-Jie Wang, Shi-Qiang Wang and Ming Xu analyzed the data. Jin-Jing Zhang, Min Zhu, Jia-Xing Wang, Shi-Qiang Wang and Ming Xu wrote the paper.

Appendix A. Supplementary data

Supplementary data to this article can be found online at https://doi.org/10.1016/j.scib.2019.05.017.

References

[1] Thum T, Condorelli G. Long noncoding RNAs and microRNAs in cardiovascular pathophysiology. Circ Res 2015;116:751–62.
[2] McManus DD, Lin H, Tanriverdi K, et al. Relations between circulating microRNAs and atrial fibrillation: data from the Framingham Offspring Study. Heart Rhythm 2014;11:663–9.
[3] Abu-Halima M, Kahraman M, Henn D, et al. Deregulated microRNA and mRNA expression profiles in the peripheral blood of patients with Marfan syndrome. J Transl Med 2018:16. https://doi.org/10.1186/s12967-018-1429-3.
[4] Heger J, Schulz R, Euler G. Molecular switches under TGFβ signalling during progression from cardiac hypertrophy to heart failure. Br J Pharmacol 2016;173:3–14.
[5] Xu M, Zhou P, Xu SM, et al. Intermolecular failure of L-type Ca^{2+} channel and ryanodine receptor signaling in hypertrophy. PLoS Biol 2007;5:e21.
[6] Takeshima H, Komazaki S, Nishi M, et al. Junctophilins: a novel family of junctional membrane complex proteins. Mol Cell 2000;6:11–22.
[7] Guo A, Wang Y, Chen B, et al. E-C coupling structural protein junctophilin-2 encodes a stress-adaptive transcription regulator. Science 2018;362:eaan3303.
[8] Wu HD, Xu M, Li RC, et al. Ultrastructural remodelling of Ca^{2+} signalling apparatus in failing heart cells. Cardiovasc Res 2012;95:430–8.
[9] Zhang C, Chen B, Guo A, et al. Microtubule-mediated defects in junctophilin-2 trafficking contribute to myocyte transverse-tubule remodeling and Ca^{2+} handling dysfunction in heart failure. Circulation 2014;129:1742–50.
[10] Chen B, Guo A, Zhang C, et al. Critical roles of junctophilin-2 in T-tubule and excitation-contraction coupling maturation during postnatal development. Cardiovasc Res 2013;100:54–62.
[11] Zhao YT, Wang M, Fu SX, et al. Small RNA profiling in two Brassica napus cultivars identifies microRNAs with oil production and development-correlated expression and new small RNA classes. Plant Physiol 2012;158:813–23.
[12] Zhang Y, Zhang W, Dong M. The miR-58 microRNA family is regulated by insulin signaling and contributes to lifespan regulation in Caenorhabditis elegans. Sci China Life Sci 2018;61:1060–70.
[13] Lv N, Hao S, Luo C, et al. miR-137 inhibits melanoma cell proliferation through downregulation of GLO1. Sci China Life Sci 2018;61:541–9.
[14] Wang M, Wu HJ, Fang J, et al. A long noncoding RNA involved in rice reproductive development by negatively regulating osa-miR160. Sci Bull 2017;7:470–5.
[15] Deng Y, Liu M, Li X, et al. microRNA-mediated R gene regulation: molecular scabbards for double-edged swords. Sci China Life Sci 2018;61:138–47.
[16] Ullrich ND, Fanchaouy M, Gusev K, et al. Hypersensitivity of excitation-contraction coupling in dystrophic cardiomyocytes. Am J Physiol Heart Circ Physiol 2009;297:H1992–2003.
[17] Benitah JP, Kerfant BG, Vassort G, et al. Altered communication between L-type calcium channels and ryanodine receptors in heart failure. Front Biosci 2002;7:e263–275.
[18] Pieske B, Maier LS, Bers DM, et al. Ca^{2+} handling and sarcoplasmic reticulum Ca^{2+} content in isolated failing and nonfailing human myocardium. Circ Res 1999;85:38–46.
[19] Zhou K, Hong T. Cardiac BIN1 (cBIN1) is a regulator of cardiac contractile function and an emerging biomarker of heart muscle health. Sci China Life Sci 2017;60:257–63.
[20] Yamazaki D, Yamazaki T, Takeshima H. New molecular components supporting ryanodine receptor-mediated Ca^{2+} release: roles of junctophilin and TRIC channel in embryonic cardiomyocytes. Pharmacol Ther 2009;121:265–72.
[21] Beavers DL, Wang W, Ather S, et al. Mutation E169K in junctophilin-2 causes atrial fibrillation due to impaired RYR2 stabilization. J Am Coll Cardiol 2013;62:2010–9.
[22] Du X. Post-infarct cardiac injury, protection and repair: roles of non-cardiomyocyte multicellular and acellular components. Sci China Life Sci 2018;61:266–76.
[23] Wu Y, Li J, Xu L, et al. Mechanistic and therapeutic perspectives for cardiac arrhythmias: beyond ion channels. Sci China Life Sci 2017;60:348–55.
[24] Zhao YT, Guo YB, Fan XX, et al. Role of FK506-binding protein in Ca^{2+} spark regulation. Sci Bull 2017;62:1295–303.
[25] Epis MR, Barker A, Giles KM, et al. The RNA-binding protein HuR opposes the repression of ERBB-2 gene expression by microRNA mir-331-3p in prostate cancer cells. J Biol Chem 2011;286:41442–54.
[26] Epis MR, Giles KM, Barker A, et al. miR-331-3p regulates ERBB-2 expression and androgen receptor signaling in prostate cancer. J Biol Chem 2009;284:24696–704.
[27] Zhao D, Sui Y, Zheng X. miR-331-3p inhibits proliferation and promotes apoptosis by targeting HER2 through the PI3K/AKT and ERK1/2 pathways in colorectal cancer. Oncol Rep 2016;35:1075–82.
[28] Cao Y, Zhang J, Xiong D, et al. Hsa-mir-331-3p inhibits VHL expression by directly targeting its mRNA 3'-UTR in HCC cell lines. Acta Biochim Pol 2015;62:77–82.
[29] Guo X, Guo L, Ji J, et al. miRNA-331-3p directly targets E2F1 and induces growth arrest in human gastric cancer. Biochem Biophys Res Commun 2010;398:1–6.
[30] Gu J, Fan YQ, Zhang HL, et al. Resveratrol suppresses doxorubicin-induced cardiotoxicity by disrupting E2F1 mediated autophagy inhibition and apoptosis promotion. Biochem Pharmacol 2018;150:202–13.

Jin-Jing Zhang received her M.M. from Shandong University in 2015. She is currently a M.D. candidate supervised by Prof. Ming Xu in Peking University Third Hospital. Her main research interest focuses on effects of microRNA on heart failure.

Shi-Qiang Wang is a professor of physiology in the College of Life Sciences, Peking University. He received a Ph.D. degree in Peking University in 1998. His research focuses on the intracellular calcium regulation of heart cells.

Ming Xu is a professor of Department of Cardiology in Peking University Third Hospital. He received a M.D. degree in Nagoya University in 2001. His research is focusing on understanding molecule mechanisms of the transition from the hypertrophy to heart failure.